UNIVERSITY OF TARTU
Faculty of Science and Technology
Institute of Technology

Mariia Novoshinskaia

Characterization of a Novel Dehydratase from the Polycyclic Aromatic Hydrocarbon (PAH) Consuming Microbe, *Polaromonas naphthalenivorans*

Bachelor's Thesis (12 ECTS)

Curriculum Science and Technology

Supervisor(s):
Research Fellow, Scott Bottoms

Tartu 2022

Characterization of a Novel Dehydratase from the Polycyclic Aromatic Hydrocarbon (PAH) Consuming Microbe, *Polaromonas naphthalenivorans*

Abstract:

Dihydroxy-acid dehydratases (DHAD) from the IlvD family are the limiting enzymes in the natural reaction pathway of the isobutanol biosynthesis. These enzymes catalyse the conversion of dihydroxyisovalerate into 2-ketoisovalerate, which is the third catalytic step in the isobutanol production pathway. However, the low biocatalytic activity of DHAD remains poorly understood. In this study, the recombinant production of DHAD from *Polaromonas naphthalenivorans* (PnDHAD) in E. coli and the catalytic specific activity of an alternative substrate, D-gluconate, were established using an analytical quantification detection method. The effect of reaction conditions on IlvD activity was determined in vitro using affinity tag purified IlvD protein. The specific activity of 6.8 units per mg (1 unit = 1 μmol/min) of purified PnDHAD was achieved at 25 °C at pH 8.0 toward 25 mM of D-gluconate. The observations may be used to investigate further the IlvD enzyme family and its application in biosynthesis.

Keywords:

Biosynthesis, biocatalysis, Dihydroxy-acid dehydratase, *Polaromonas naphthalenivorans*, IlvD family, isobutanol, dihydroxyisovalerate, 2-ketoisovalerate, D-gluconate, biofuels

CERCS:

1490 Biotechnology; P310 Proteins, enzymology

Polutsuklilisi süsivesikuid tarbivast mikroobist Polaromonas naphthalenivorans pärit uudse dehüdrataasi iseloomustamine

Lühikokkuvõte:

Looduses on isobutanooli biosünteesirajas piiravaks etapiks IlvD perekonna dihüdroksühappe dehüdrataaside (DHAD) poolt läbiviidav reaktsioon, mille käigus muudetakse dihüdroksüvaleraat 2-ketoisovaleraadiks. See on isobutanooli biosünteesirajas 3. etapp. Praegu ei ole teada, mis on DHAD madala katalüütilise aktiivsuse põhjus. Käesolevas töös koloneeriti, ekspresseeriti E. coli’s ja puhastati Polaromonas

naphthalenivorans'i dihüdroksuhappe dehüdrataas (PnDHAD), mida seni uuritud ei ole. Lisaks, kasutades HPLC põhist meetodit, teostati ensüümi PnDHAD spetsiifilise aktiivsuse määramine dihüdroksüvaleraadi analoogi D-glükonaadi suhtes. Töö käigus uuriti reaktsioonitingimuste mõju ensüümi aktiivsusele. Katsete tulemusena selgitati välja, et PnDHAD spetisiifliseks aktiivsuseks 25°C, pH 8.0, 25mM D-glükonaadi juuresolekul on 6.8 ühikut mg puhastatud valgu kohta. Saadud tulemused annavad lisainfot IlvD ensüümiperekonna valkude katalüütiliste omaduste kohta ning võimaldavad edasi uurida nende kasutamist isobutanooli biosünteesis.

Võtmesõnad:

Biosüntees, biokatalüüs, dihüdroksü-happedehüdraas, *Polaromonas naphthalenivorans*, IlvD perekond, isobutanool, dihüdroksüisovaleraat, 2-ketoisovaleraat, D-glükonaat, biokütused

CERCS:

T490 Biotehnoloogia; P310 Proteiinid, ensümoloogia

TABLE OF CONTENTS

LIST OF FIGURES

LIST OF TABLES

TERMS, ABBREVIATIONS AND NOTATIONS

AtJ – Alcohol-to-Jet fuels

DHAD – Dihydroxy-acid dehydratase

GHG – Greenhouse gas

LB medium – lysogeny broth medium

LCB – Lignocellulosic biomass

PAH – Polycyclic aromatic hydrocarbon

PCR – Polymerase chain reaction

UNFCCC – United Nations Framework Convention on Climate Change

2,3-KDG – 2-Keto-3-deoxy-D-gluconate

INTRODUCTION

Nowadays, greenhouse gas (GHG) emission remains one of the most significant global challenges leading to climate change. To address this problem and reduce the number of air pollutants, society is establishing ways to limit GHG emissions. One of the main strategies is to substitute non-renewable fossil fuels with renewable biofuels, as fossil fuels are the primary sources of GHG production. Biofuels are cheap and ecologically friendly alternatives to fossil fuels, produced from biological sources, such as raw biomass or feedstocks. Isobutanol is a biofuel produced from lignocellulosic biomass (LCB) during the fermentation process. Various microorganisms, such as yeasts and bacteria, can be used for LCB fermentation.

The critical mechanism enabling isobutanol production in fermentation is bacterial pyruvate synthesis. Pyruvate-to-isobutanol pathway in yeasts consists of five enzymatic reactions. The speed and amount of the isobutanol production depend on the activity of each enzyme class involved in the process.

In this study, we focus our attention on the IlvD enzyme family. The IlvD protein family includes dihydroxy-acid dehydratases (EC 4.2.1.9), which participate in the pyruvate-to-isobutanol pathway. These enzymes can convert the (2R)-2,3-dihydroxy-3-methyl butanoate (2,3-dihydroxy isovalerate; common synonym) into the 3-methyl-2-oxobutanoate (2-ketoisovalerate; common synonym) by dehydrating the initial product. However, the biochemical properties of this enzymatic family remain poorly studied. To enhance bioconversion efficiency, it is essential to determine the properties of the IlvD enzymatic class.

1 LITERATURE REVIEW

1.1 Climate change problem

Of the most significant challenges for modern society is climate change. To guarantee a habitable environment for future generations, the world is identifying ways to save our planet from the rising risk of global warnings due to the emission of greenhouse gas (GHG). Greenhouse gas, or carbon dioxide, collects heat after being released into the atmosphere leading to global warming. To address climate change issues and establish strategies to stabilize the GHG levels in the atmosphere, a particular organization – United Nations Framework Convention on Climate Change (UNFCCC), was created. UNFCCC was formed during the United Nations Conference in Rio de Janeiro in 1992 (*About the Secretariat | UNFCCC*, n.d.).

1.1.1 Kyoto protocol

Kyoto protocol is the first document providing legally enforceable requirements for greenhouse gas emissions, reductions, and limitations. This document was used from 2008 to 2012 and 2013 to 2020 (*What Is the Kyoto Protocol? | UNFCCC*, n.d.).

This document puts the UNFCCC into action requiring developed countries to reduce and limit greenhouse gas emissions following the agreed-upon terms. Participating countries must implement mitigation policies and measures to reduce and limit GHG emissions and report on them regularly.

During the first commitment period (2008-2012), the Kyoto Protocol arranged emission reduction goals totaling a 5% reduction in emissions. The obtained results contrasted with the levels in 1990 (*What Is the Kyoto Protocol? | UNFCCC*, n.d.).

This document was established on the UNFCCC's provisions and principles, and it operates under the convention's annex-based structure. Furthermore, the protocol is only binding on developed countries, imposing a more significant burden on them under the principle of common but differentiated responsibility and respective capabilities (*What Is the Kyoto Protocol? | UNFCCC*, n.d.).

The Kyoto Protocol only binds developed countries because the convention recognizes that these countries are primarily responsible for the prominent levels of greenhouse gases.

In 2012, changes known as Doha Amendment were added to the Kyoto protocol (*What Is the Kyoto Protocol? | UNFCCC*, n.d.). New adjustments included:

- New requirements for the countries participating in the second commitment period
- An updated GHG list of which parties should cover during 2013-2020
- Different changes in the Kyoto protocol articles covered the 2008-2012 period and needed to be updated.

Implementing these amendments to the Kyoto Protocol was a significant step toward maintaining sustainable GHG levels during the second commitment period.

1.1.2 Paris agreement

The Paris agreement was adopted during the 21st UNFCCC Conference of the Parties in Paris in 2015. This agreement intends to reduce global GHG emissions to prevent global temperatures from rising. The aims are to limit global temperature increases to below 2 °C above preindustrial levels. By signing the Paris Agreement, developing countries were given a chance to fight against global warming, together with developed ones. At the moment, every country on the planet has become a part of this agreement (*The Paris Agreement | UNFCCC*, n.d.).

The central goals for the Paris Agreement were:

- Minimizing the adverse effects of climate change by limiting the increase of global temperatures because of the reduction of greenhouse gas emissions
- Creation of a framework that will allow achieving higher goals
- Assist developing countries in averting climate change and coping with its adverse effects

The Paris Agreement requires every participating country to set its own goals after five years (*The Paris Agreement | UNFCCC*, n.d.). The Kyoto protocol declares a standard set of targets and does not specify a timeline to achieve them.

1.2 Linear economy model versus Circular economy model

Replacing the linear economy with a circular economy is the primary goal of protecting the environment. The linear economy model is the oldest economic model, also called as take-

make-dispose strategy, and is still currently the world's prevailing economic pathway. The linear model relies on the concept of naturally derived materials, which are later converted into final products of interest. After they have been used, their leftovers are disposed of in the environment (Neves & Marques, 2022). For example, the primary sources used in the linear economic strategy for a product design are fossil-based oil and coal. Such products cannot be reused, as they have been designed for single-use and have a short life period. Waste generated because of linear strategy application could not be further utilized.

The circular economy is based on reusing products rather than scrapping them and extracting novel resources, as done in a linear economy (**Figure 1**) (*Circular Economy | UNCTAD*, n.d.).

A circular economy involves replacing fossil-based carbon resources with renewable carbon ones. Implementing renewable energy sources is essential since fossil-based energy sources – such as natural gas, coal, and oil – are non-refundable, and their usage causes dramatic changes to Earth's climate. When fossil sources are burned, greenhouse gasses are released into the atmosphere, and little technology is available to recover the carbon gas from the atmosphere. The more fossil fuels are burned, the worse GHG emissions are.

Renewable energy sources allow us to reach a more sustainable energy system where carbon emissions almost do not exist.

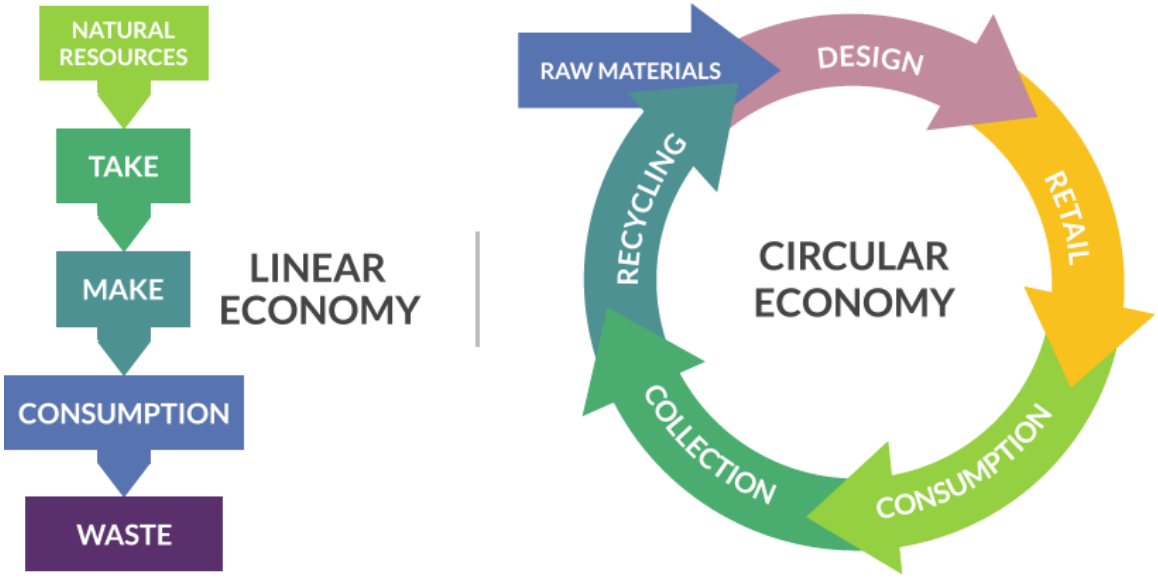

Figure 1. Differences between linear and circular economy.

(*MVIS | MVIS OneHundred - A Circular Economy: Designing out Waste*, n.d.)

1.3 Biofuels

Biofuels are an excellent substitution for traditional fossil carbon energy sources. These, for example, ethanol and biomass-based diesel, are fuels made from raw biomass resources or feedstocks.

The feedstock is an essential part of the creation of biofuels. First-generation biofuels are made from food crops and create the majority of the biofuels used nowadays (Dahman *et al*., 2019). For example, ethanol is an alcohol made from sugars in corn or rice, an example of first-generation biofuels (Kang & Lee, 2015). However, human food sources produced non-sustainable biofuels in first-generation biofuels (Mohr & Raman, 2013).

Another way to create biofuels is to use a lignocellulosic material composed of carbohydrate polymers, such as cellulose or hemicellulose, and lignin, an aromatic polymer (Chen, 2015). Second-generation biofuels are produced this way. Cellulose is further broken down into C6 sugars - glucose, galactose, and mannose. Hemicellulose is broken down into C5 sugars – xylose, arabinose, and ribose. These sugars can convert into other substances as the primary source of biofuels. For example, a pathway allows the conversion of glucose to pyruvate – glycolysis (Harris, 2013). In this study, the pathway to convert pyruvate to isobutanol is of most interest (Noda *et al*., 2019).

1.3.1 Methods to convert sugars into biofuels

As has been already mentioned above, biofuels, such as ethanol and biodiesel are made from sugars. The fermentation of biomass produces ethanol, and the chemical trans-esterification of plant oil creates biodiesel (Kang & Lee, 2015). Since lignocellulosic biomass (LCB) is the most suitable source for ethanol production, as it does not compete with human and animal feeding demands, fermentation of lignocellulosic material to ethanol is one of the ways to create supplements for fossil fuels. This biomass can be taken from leftovers of the wood industry, which significantly shortens the amount of waste (Gutiérrez-Antonio *et al*., 2021).

1.3.2 Drop-in and Alcohol-to-Jet biofuels

There are several types of biofuels. Drop-in biofuels or renewable hydrocarbon fuels are produced from biomass sources through biological, chemical, and thermal processes. Drop-in biofuels can replace petroleum fuels and be used in engines or infrastructure. The main feature of renewable hydrocarbon fuels is that they can be blended with petroleum products

and later utilized with current infrastructure without any modern technologies and equipment (*Alternative Fuels Data Center: Renewable Hydrocarbon Biofuels*, n.d.).

Biofuel of such type involves a gasoline blender obtained from distinct gasoline stocks to form the fuel's base. Butanol, terpenes, and isoprene are examples of drop-in fuels defined in this way. Rather than gasoline, the technology is frequently applied to diesel fuel, resulting in biodiesel. Some proponents of next-generation biofuels are even developing chemical mixtures to create a biofuel without gasoline or diesel.

Another type of biofuels is called Alcohol-To-Jet fuels (AtJ), which are jet fuels obtained by dehydration of alcohols followed by oligomerization, then hydrogenation and polymerization into various kinds of paraffin. The aviation industry needs sustainable alternatives to regular jet fuels to reduce GHG emissions because they are essential to reducing the environment's harmful impact. Moreover, AtJ fuels will allow reducing the dependence of the aviation industry on foreign sources of oil (Geleynse *et al*., 2018).

1.3.3 Ethanol

Ethanol is a first-generation biofuel that can be made from biomass. Ethanol can be produced either from food or non-food feedstocks (Kang & Lee, 2015).

The first type of ethanol is primarily produced using the dry mill technology – a process where corn is firstly ground into the flour. Then the starch is fermented into ethanol (Brito Cruz *et al*., 2014). About 90% of ethanol is made this way. Ethanol, produced this way, is biodegradable, but it negatively affects food production, as it takes an enormous amount of corn to produce ethanol from it. As the demand for corn-based ethanol increases, the number of agricultural lands will be used to plant corn, which will negatively impact the production of other crops (Elobeid *et al*., 2006).

Another type of ethanol is produced from non-food feedstocks, such as waste products or specially grown as energy sources crops harvested from lands not suitable for other plants. Examples of such cellulosic stocks are switchgrass and corn stover. There are many challenges in collecting, harvesting, and delivering such stocks, so currently, cellulosic ethanol is produced and sold in minimal amounts (Krishnan *et al*., 2020).

Moreover, ethanol has only 70% of the energy content of petrol (Kang & Lee, 2015), and it also has a high tendency to absorb water from the air, which can be the reason for corrosion in engines and pipes (Baroš *et al*., 2022).

1.3.4 Isobutanol

Isobutanol is a second-generation biofuel. It has significant advantages over ethanol as a fuel as it has 26% more energy. Unlike ethanol, isobutanol has limited solubility because it is produced via dehydration, and it also does not lead to the breakage of engines and pipes. Besides, isobutanol can be easily blended into gasoline due to its low oxygen content (Brownstein, 2015). Nowadays, isobutanol is considered an advanced biofuel under the Re-formulated Fuel Standard (Demirel, 2018). Isobutanol can be produced in the process of fermentation with genetically modified organisms (Kang & Lee, 2015; Peralta-Yahya *et al*., 2012) and even *in vitro* synthesized from glucose in a bioreactor (Sherkhanov *et al*., 2020). Also, isobutanol is a type of biofuel, which can be produced from lignocellulosic material (Lakshmi *et al*., 2021), for example, waste stocks left from the wood industry, leftovers from crop production industries, or already existing cornstarch ethanol fermentation plants. This fuel production technology offers reduced cost in the production itself and lower risks of adverse effects on the environment among with the reduction of GHG effect.

1.3.5 Pyruvate fermentation to isobutanol pathway

Some yeast strains produce isobutanol as a by-product of fermentation (Wess *et al*., 2019). After glycolysis, once the pyruvate stage is reached, the pathway of isobutanol fermentation from pyruvate involves five major steps. Each step is a different enzymatic reaction involving different enzymes (*Pyruvate Fermentation to Isobutanol (Engineered)* | *Pathway - PubChem*, n.d.).

The first step is a reaction of conversion of 2-pyruvate into (S)-2-acetolactate by enzymes from the synthase class (EC. 2.2.1.6) when the (S)-2-acetolactate is converted into the (2R)-2,3-dihydroxy-3-methyl butanoate with the presence of oxidoreductase (EC 1.1.1.86) enzymes. The third step in this pathway is a convertion (2R)-2,3-dihydroxy-3-methyl butanoate into the 3-methyl-2-oxobutanoate with enzymes from the dehydratase class (EC 4.2.1.9). This enzyme class is of primary interest in the present work. The reaction at the fourth step involves enzymes from the decarboxylase class (EC 4.1.1.72), which convert the 3-methyl-2-oxobutanoate into the isobutanal. The final step in the pathway is a conversion of isobutanal into isobutanol by a class of enzymes from the dehydrogenase class (EC 1.1.1.1) (**Figure 2**).

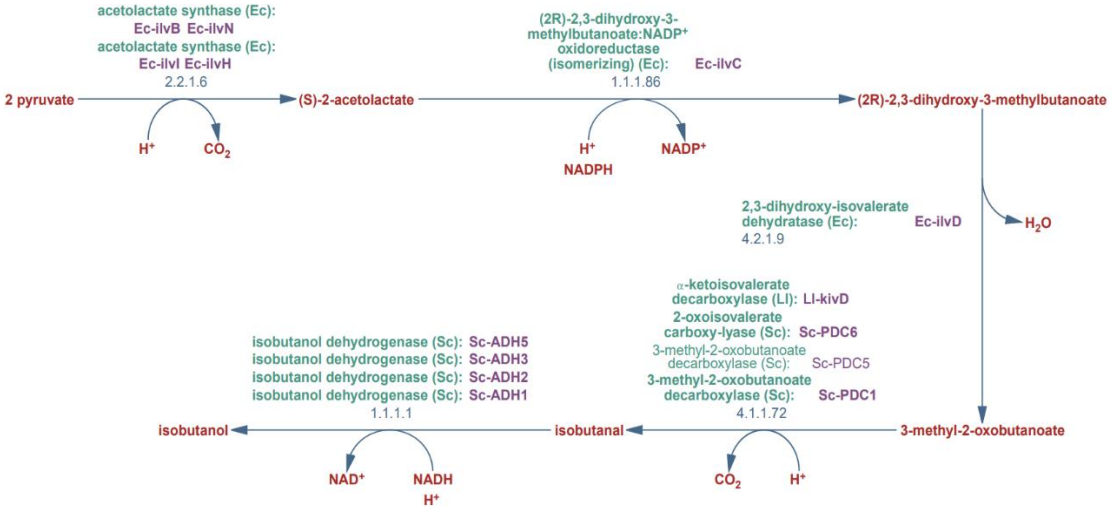

Figure 2. Engineered pathway: pyruvate fermentation to isobutanol.

(Caspi *et al*., 2018)

1.4 *Polaromonas naphthalenivorans*

Polaromonas naphthalenivorans are proteobacteria capable of aerobic degradation of naphthalene, a polycyclic aromatic hydrocarbon (PAH). Naphthalene can be toxic or carcinogenic. *P. naphthalenivorans* was discovered and described in 2004 by Jeon, C. O. It was isolated from coal-tar-contaminated freshwater sediment in South Glens Falls, New York, USA (Jeon *et al*., 2004). The usage of this particular microbe in this study is applicable because its genome contains several dihydroxy-acid dehydratases (DHAD) enzymes. The DHAD enzyme was cloned and expressed using the synthetic biology techniques described below.

1.5 Dihydroxy-acid dehydratases

1.5.1 Dehydratases

The dehydratases are a class of lyases that form double and triple bonds with the substrate by removing water. Dehydratases catalyse the breakage of a carbon-oxygen bond that leads to the formation of unsaturated products (Singh *et al*., 2019). The dehydratases are limiting enzymes in the reactions with low specific activities.

1.5.2 Dihydroxy-acid dehydratases

Dihydroxy-acid dehydratases (DHAD) are enzymes that catalyse the dehydration of (2R, 3R)-2, 3-dihydroxy-3-methyl pentanoate (2,3-dihydroxy-3-methyl valerate) into 2-oxo-3-3-methyl pentanoate (2-oxo-3-methyl valerate) and of (2R)-2,3-dihydroxy-3-methyl butanoate (2,3-dihydroxyisovalerate) into 2-oxo-3-methyl butanoate (2-ketoisovalerate), the penultimate precursor to L-isoleucine and L-valine, respectively (*ENZYME - 4.2.1.9 Dihydroxy-Acid Dehydratase*, n.d.; MYERS, 1961).

Dihydroxy-acid dehydratases from *Polaromonas naphthalenivorans* belong to the IlvD enzyme family. IlvD enzymes, along with many other dehydratases, contain the iron-sulfur ([Fe-S]) cluster (Gao *et al*., 2018). This cluster assists in substrate binding and enables catalysis by providing a local positive charge. Moreover, the presence of an iron-sulfur cluster allows the net dehydration of a substrate (Imlay, 2006). DHAD enzymes, containing [Fe-S] clusters, are dependent on the metal ions as they are co-factors to the enzyme activity (Rahman *et al*., 2017).

Many enzymes from this family are used in the biosynthesis of valuable chemicals. In this study, three novel dehydratases from the IlvD family – WP_011802045.1 (IlvD11), WP_011802252.1 (IlvD17), and WP_011801097.1 (IlvD19) are investigated. Each one may have different activities on different substrates. One may be highly active on C6 acid-sugars, such as glucose and galactose, while another may be highly active on C5 acid-sugars, such as xylose and arabinose. All these sugars can be found in the lignocellulosic stoks which are used in the biofuels production. At least one of these dehydratases may be used more efficiently in isobutanol biosynthesis.

2 THE AIMS OF THE THESIS

The aims of this work are:

- Isolate and clone genes from *P. naphthalenivorans* encoding putative dihydroxy-acid dehydratases (DHAD) enzymes into expression vectors.
- Using *E. coli* BL21 DE3 cells, specially designed for protein expression, express DHAD from expression plasmids.
- Examine enzymatic activities of expressed DHADs on an alternative substrate.

3 EXPERIMENTAL PART

3.1 MATERIALS AND METHODS

3.1.1 Bacteria strains

E. coli Turbo cell strain (New England Biolabs) was used for the first bacterial transformation. Heterologous expression of DHAD occurred in the bacterial strain *E. coli* BL21-DE3s. Both strains were provided by the LoogLab.

Polaromonas naphthalenivorans (DSM 15660) genomic DNA used in this study was ordered from the DSMZ.

3.1.2 Primer design

Two specific primers were designed- forward and reverse primers for each of the three *P. naphthalenivorans* genes of interest (IlvD11, IlvD17, and IlvD19). Different restriction sites were used: NdeI and XhoI for genes IlvD11 and IlvD19, and NheI and XhoI for IlvD17. Primer characteristics are defined in the attached table (**Table 1**).

Table 1. Primer characteristics. The table contains primer names, specific melting temperatures (in °C), length, and structure information.

Primer name	Primer	Melting Temperature	Length
11_ilvD_NdeI_fwrd	atatatcatatgATGACTAAAAAAACCTACGCGG	56	34-mer
11_ilvD-XhoI_rvrs	tatatactcgagTCAATAGATGTCGGGCTCGCC	58	33-mer
17_ilvD_NheI_FW	atatatgctagcATGTCTCCTACCCCAAAACG	57	32-mer
17_ilvD_XhoI_rvrs	tatatactcgagTTAATGGGAATGACGCGGAACC	58	34-mer
19_ilvD_NdeI-FW	atatatcatatgATGGAAACCAAAGTCATCGC	56	32-mer
19_ilvD_XhoI-RV	tatatactcgagTCAATAGTCATCAAGCACCGC	55	33-mer

3.1.3 Plasmid construct

Plasmids constructed in this work were based on the pET-28a vector containing lac-operon.

3.1.4 PCR amplification of plasmids

Polymerase chain reaction (PCR) was performed with two different three-step specifically designed programs in the thermolcycler. The 11-17_IlvD program was designed to amplify 11IlvD and 17IlvD genes from *Polaromonas naphthalenivorans* with 11_ilvD_NdeI_fwrd, 11_ilvD-XhoI_rvrs, 17_ilvD_NheI_FW, and 17_ilvD_XhoI_rvrs. 19_IlvD program was performed to amplify *Polaromonas naphthalenivorans* 19IlvD gene with 19_ilvD_NdeI-FW 19_ilvD_XhoI-RV primers. Program settings are described in the attached tables (**Table 2**,

Table 3). Each PCR mixture reagent and its final concentrations are described in **Table 4**. The final volume of each PCR mixture was 50 µL. The length of the amplifying region determined the extension time for each program. The annealing temperature is calculated by taking the composition and length of the primers into consideration. After PCR was performed, every PCR mixture was stained with 6x Orange DNA Loading Dye (Thermo Fisher Scientific) and loaded onto 1% Agarose gel (1% Agarose, 1x TAE buffer and 0,5 µL DNA dye). Gel electrophoresis was done in 1x TAE buffer. Together with the PCR mixtures, GeneRuler DNA Ladder 1 (Thermo Fisher Scientific) was loaded into the gel to enable further detection of fragments' lengths under UV light. The correct size bands were cut from the gel, placed into separate 1.5 mL tubes, and later purified. According to the manufacturer's instructions, amplified 11IlvD, 17IlvD, and 19IlvD fragments were purified from the gel with FavorPrep™ GEL/PCR Purification Kit (Favorgen) according to the instructors provided by the manufacturer. At the last step of the gel purification process, elution buffer was substituted with Milli-Q H_2O.

Table 2. Three-step PCR program "PCR_11_17_IlvD ". PCR cycles are constructed for plasmid amplification.

Step	Temperature	Time	Number of cycles
Initial Denaturation	98°C	3 min	1
Denaturation	98°C	60 s	30
Annealing	58°C	10 s	30
Extension	72°C	1 kb/60 s	30
Final Extension	72°C	10 min	1

Table 3. Three-step PCR program "PCR_19_IlvD ". PCR cycles are constructed for plasmid amplification.

Step	Temperature	Time	Number of cycles
Initial Denaturation	98°C	3 min	1
Denaturation	98°C	60 s	30
Annealing	56°C	10 s	30
Extension	72°C	1 kb/60 s	30
Final Extension	72°C	10 min	1

Table 4. PCR mixture. Components of PCR mix and their concentrations.

Reagent	Final concentration
DNA template	0,5 ng/µL
5x Phusion HF Buffer	10 µL (1x)
Forward primer	1 µL
Reverse primer	1 µL
dNTPs	0,5 µL
High-fidelity Phusion DNA Polymerase	0,5 µL
Milli-Q H2O	Up to 50 µL

3.1.5 Restriction digestion

Before starting the digestions, the concentration of each purified, amplified insert was measured with Thermo Fisher's NanoDrop 1000 Spectrophotometer. Amplified inserts needed to be digested with the corresponding enzymes to be prepared for the future vector

(pET 28-a) integration. Primers, designed specifically for each of the genes, contained corresponding cutting sites, enabling the restriction of the enzyme of interest. Furthermore, the vector of choice (pET 28-a) also had to be digested with the same restriction enzymes as the inserts to enable future ligation. Digestion procedures were performed with restriction enzymes – XhoI, NdeI, and NheI. XhoI restriction enzyme was used for each insert, NdeI was used for 11IlvD and 19IlvD enzyme inserts, and NheI was used for the 17IlvD enzyme insert. The digestion mixture reagents and their final concentrations are described in **Table 5**. The final volume of each digestion mixture was 10 µL. Mixtures were incubated for 60 minutes at 37°C. After 30 minutes from the start, all tubes were spun down to pellet the condensate. Once the incubation was over, all mixtures were incubated at 60°C for 20 minutes to inactivate the nucleases. After the heat inactivation, a mixture containing linearized pET 28-a vector and mixtures containing amplified inserts were purified and cut with preqGOLD Plasmid Miniprep Kit I (VWR). Their concentrations were later measured with Thermo Fisher's NanoDrop 1000 Spectrophotometer.

Table 5. Digestion mixture. Components of the digestion mixture and their final concentrations.

Reagent	Final concentration
Vector (pET 28-a) or PCR amplified insert	1 µL
Restriction enzymes (x2)	1 µL
10x FastDigest™	1 µL
Milli-Q H2O	Up to 10 µL

3.1.6 Ligation

After vector and gene inserts are digested with the same enzymes, they need to be ligated together. Contents of the ligation mixture are described in **Table 6**. The final volume of each ligation mixture was 20 µL. Every ligation mixture was incubated at 25°C for 50 minutes.

Table 6. Ligation mixture. Components of the ligation mixture and their final concentrations.

Reagent	Final concentration
Vector (pET 28-a)	50 ng
PCR amplified inserts	0,5 µL
T4 ligase	1 µL
10x ligation buffer	2 µL
ATP	0,5 µL
Milli-Q H2O	Up to 20 µL

3.1.7 Bacterial transformation and plasmid verification

The bacterial transformation was performed to receive a higher number of ligated plasmids. In this process, *E.coli* Turbo cell strain (competed cells) was used. Firstly, cells were taken from the -80°C and placed on ice for 30 minutes to thaw. 50 µL of competent bacteria cells were mixed with 2 µL of ligation mixture in the new tube and then resuspended. After the tube was placed on ice for 30 minutes. Later, the Heat shock was performed – the tube was incubated at 42°C for 30 seconds and then placed back on the ice for 5 minutes. 600 µL of LB media ontaining kanamycin (100x) was added to the tube, and the tube was then incubated at 37°C for 60 minutes in the shaker. Afterward, 125 µL of the mixture was plated on the pre-heated at 37°C LB plate containing kanamycin. Cells were left to overnight growth at 37 °C. The same procedure was performed on the amplified gene – IlvD11, Ilvd17, and IlvD19. Cells were plated on the separate LB+Kanamycin agar plates.

After the overnight growth, two colonies from each plate were taken and grown in the separate 15 mL flasks with 5 mL of liquid LB media with 1000 µg/mL kanamycin. Flasks were incubated in the shaker at 30°C overnight. The next day, PCR and gel electrophoresis for each cell mixture were performed to detect if plasmids had uptaken desired inserts. PCR program and gel electrophoresis procedure remain the same as previously described. Program settings are described in the attached tables (**Table 2**, **Table 3**). Each PCR mixture reagent and its final concentrations are described in **Table 4**. The final volume of each PCR mixture was 50 µL. After PCR was performed, every PCR mixture was stained with DNA

loading buffer and loaded onto 1% Agarose gel (add gel reagents). Gel electrophoresis was done in 1x TAE buffer.

Together with the PCR mixtures, DNA Ladder 1 (Thermo) was loaded into the gel to enable further detection of fragments' lengths under UV light. Cell colonies in which plasmids contained plasmids of interest were marked as colonies of interest. Cell mixtures containing correct cells with 300 μL and 100x kanamycin were re-plated on the already pre-heated at 37°C LB plate containing kanamycin. Cells were left to overnight growth at 37 °C. The same procedure was performed on the amplified gene – IlvD11, Ilvd17, and IlvD19. Cells were plated on the separate dishes. The next day, plasmids of interest were purified from the separate colonies from each gene plate. Plasmids were purified with preqGOLD Plasmid Miniprep Kit I (VWR) according to the manufacturer's instructions. Purified plasmid stocks were frozen at -20°C.

3.1.8 Plasmid transformation into the BL21-DE3s bacteria

Plasmids were sent for the Sanger sequencing before being transformed into *E. coli* BL21-DE3s bacteria strain. The BL21-DE3s strain was used as it is capable of high rate protein expression. Before starting the bacteria transformation, BL21-DE3s cells were taken from the -80°C and placed on ice for 30 minutes to thaw. 50 μL of bacteria cells were mixed with 2 μL of purified plasmid mixture in the new tube and then gently flipped over a couple of times. After the tube was placed on ice for 20 minutes. Later, the Heat shock was performed – the tube was incubated at 42°C for 45 seconds and then placed back on the ice for 5 minutes. Later, 1 mL of LB media was added to the tube, and the tube was then incubated at 37°C for 60 minutes in the shaker. Afterward, 125 μL of the mixture was plated on the pre-heated at 37°C LB plate containing kanamycin. Cells were left to overnight growth at 37°C. The same procedure was performed on the amplified gene – IlvD11, Ilvd17, and IlvD19. Cells were plated on the separate dishes.

3.1.9 Buffer preparation

During the protein expression and purification processes, three different buffers were made and, when used, elution buffer, binding buffer, and HEPES pH 8.0 buffer. 1L of binding buffer consists of 500 mM NaCl, 20 mM imidazole, 10% glycerol, and 50 mM KPi pH 8.0 buffer, 1L of which was composed of 0,047 M Potassium phosphate dibasic (K_2HPO_4) and 0,003 M Potassium phosphate monobasic (KH_2PO_4). 1L of elution buffer 500mM NaCl, 500 mM imidazole, 10% of glycerol, and 50 mM KPi pH 8.0. 1L of HEPES buffer with pH 8.0

was made with 1 M HEPES (Sigma-Aldrich) and Milli-Q H_2O, 10N NaOH was used to adjust solution to the desired pH level. The reason why imidazole concentrations vary between the buffers is that binding buffer (also reffered as a wash buffer) is used to reduce non-specific binding events during protein purification experiment and elution buffer is mainly needed to release the His-tag with the protein of ineterst from the column.

3.1.10 Expression and purification of DHAD

Expression and purification of enzymes of interest were done twice. Once plasmids containing pET 28-a vector and genes of interest were transformed to the BL21-DE2s *E. coli* strain, plated, and individual colonies were grown on each plate, cells were needed to be prepared for the protein expression. During the first try, one individual colony from each plate was taken and grown in the separate 250 mL flasks with 50 mL of liquid LB media with 1000 μg/mL kanamycin in each. Flasks were incubated in the shaker at 37°C, 200 rpm for 24 hours. When the enzymes were expressed in the 1L of the auto-induction media, the contents are described in **Table 7**, with 500 mL. Cells were cultivated at 37 °C, 160 rpm for 3 hours, and after the temperature was decreased to 16 °C, the speed was decreased to 90 rpm. The culture was in these conditions for 18 hours. During the second experimental setup, the procedure was the same as during the first attempt, except for the content of the autoinduction media, which is described in **Table 8**.

In both experiment setups, cells were harvested by centrifugation (6,000 rpm, 30 min, 10 °C), and cell pellets were resuspended with 40 mL binding buffer and then frozen at -20 °C. After cell pellets were disrupted by sonication, crude cell lysates were centrifuged (12,000 rpm, 30 min, 4 °C) to remove cell debris. Later, the His-tagged DHAD proteins were purified from the supernatant using the Nickel-Iodine-Agarose (Sigma-Aldrich) affinity column via washing the cell lysate through the columns with binding and elution buffers. After the purification procedure, samples are desalted to remove the imidazole. The salt removal procedure was performed using desalting columns (Thermo Scientific (old Pierce) Zeba Columns). Protein concentrations were measured with Thermo Fisher's NanoDrop 1000 Spectrophotometer.

Table 7. Autoinduction media composition. Components of an autoinduction media used during the first experimental setup and their final concentrations.

Reagent	Final concentration
ZY media	958 mL
50x M	20 mL
50x 5052	20 mL
Trace elements (solution was provided by supervisor)	200 µL
1 M $MgSO_4$	2 mL

Table 8. Autoinduction media composition. Components of an auto-induction media used during the second experimental setup and their final concentrations.

Reagent	Final concentration
ZY media	958 mL
50x M	20 mL
50x 5052	20 mL
Trace elements	200 µL
1M $MgSO_4$	2 mL
1M $FeCl_2$	2 mL

3.1.11 Analytical procedure

The DHAD activity was measured by high-pressure liquid chromatography (HPLC) technology. HPLC measurements were performed on a Shimadzu LC2030C 3D Plus equipped with an autosampler, diode array detector, and refractive index detector. Chromatographic separation of D-gluconate and 2,3-KDG was achieved on a Phenomenex Rezex RHM-monosaccharide column at 45 ^{O}C by isocratic elution of 0.5 mL/min with 0.5

mM H_2SO_4 with 10% Acetonitrile followed by a water washing step. Standard curves were assembled to detect the substrate and product with seven concentration points at 0.078, 0.156, 0.313, 0.625, 1.25, 2.5, and 5.0 mM of D-gluconate and 2,3-KDG.

3.1.12 DHAD activity assay method

DHAD activity assay method was performed twice. For the first experiment, the reaction mixture was divided into six 1.5 mL tubes, each containing 100 µl of 100 mM HEPES buffer pH 8.0, 90 µl MQH_20, 10 µl of 1 M $MgCl_2$, 100 µl of 100 mM D-gluconate, and 100 µl of the affinity-purified enzyme, was incubated at 37 °C for 3 hours. Time-point samples were taken six times. The first sample was taken at the start of the experiment, 20 minutes, 40 minutes, 1, 2, and 3 hours. All the samples were filtrated and then frozen at -20 °C.

During the second try, the reaction mixture was divided into seven 1.5 mL tubes, which consisted of 50 µl of 100 mM HEPES buffer with pH 8.0, 45 µl MQH_20, 5 µl of 1M $MgCl_2$, 50 µl of 100 mM D-gluconate, and 50 µL of purified enzyme solution that was incubated at 25 °C for 24 hours. Time-point samples were taken seven times at times 0, 20 and 40 minutes, 1, 2, 3, and 24 hours from the start of the experiment. All the samples were also filtrated and then frozen at -20 °C.

The enzyme activity in both cases was defined as the amount of substrate, D-gluconate, that was converted into the product, 2-Keto-3-deoxy-D-gluconate (2-3-KDG). Detection occurred as previously described above.

3.1.13 Enzyme characterization

The enzyme activity was tested twice, at 25 °C and 37 °C. For the first experiment, we decided to set experimental temperature conditions to 37 °C because other studies on enzymes from the IlvD family showed that for some of the enzymes the highest activity is achieved at 30 °C (Jiang *et al*., 2015). We wanted to keep the temperature higher to see how it would influence the activity of the IlvDs. Furthermore, DHADs we are working with are derived from *P. naphthalenivorans*, whose optimal growth conditions range from 4°C to 25°C (Jeon *et al*., 2004). To test enzymatic activity under its optimal conditions, we set our second experiment's temperature to 25 °C.

3.2 RESULTS

Polaromonas naphthalenivorans (*Pn*)DHAD-ilvD19 was cloned as described in Section 3.0 and recombinantly expressed *Pn*DHAD in *E. coli* BL21 DE3 containing an affinity his-tag enzyme yielded 7.31 mg/mL and 3.13 mg/mL across two separate purifications.

3.2.1 Determination of enzyme properties

In the first experimental set, 1.828 mg/mL of *Pn*DHAD-ilvD19 (MW 59,237.3 Da. and the extinction coefficient of 41870 was estimated using ProtParam at expasy.org) was examined for enzymatic activity on 25 mM of D-gluconate at 37 ^{O}C pH 8.0. No activity was observed under these conditions (**Figure 3**). Since other DHADs are active at pH 8.0 and similar substrate concentrations (Jiang *et al*., 2015), it was decided to purify the enzyme again and change the reaction temperature. Since *P. naphthalenivorans* was initially isolated from coal-tar-contaminated freshwater sediment (Jeon *et al*., 2004), it seemed logical to set the reaction temperature within the range of that environment. Therefore, in the second experimental set, 0.783 mg/mL of affinity tag purified *Pn*DHAD-ilvD19 was evaluated at 25 ^{O}C at pH 8.0 on 25 mM of D-gluconate. This reaction yielded a catalytic conversion of 12.86 mM of D-gluconate at 25 ^{O}C at pH 8.0 per hour for one hour with a specific activity of 6.85 μmol/min/mg enzyme becomes catalytically less active after one hour. During the second hour of the enzyme reaction time, the specific activity drops from 6.85 μmol/min/mg to 0.51 μmol/min/mg. Inactivity of the enzyme occurs between 2 and 3 hours with no measurable activity through 24 hours of the experiment (**Figure 4**, **Figure 5**). The specific activity of the 19IlvD enzyme was calculated from the amount of D-gluconate converted into 2,3-KDG at 25 ^{O}C at pH 8.0 after an hour of the reaction.

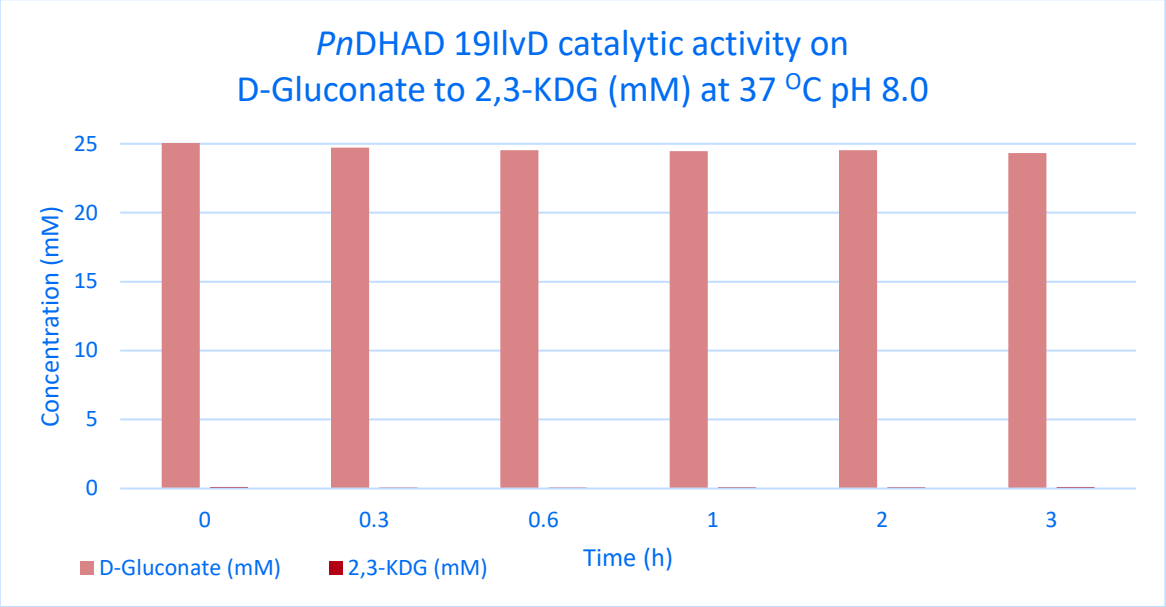

Figure 3. *Pn*DHAD 19IlvD catalytic activity on D-Gluconate to 2,3-KDG (mM) at 37 ^{O}C pH 8.0.

The data shown in the **Figure 3** corresponds to the first enzymatic activity assay results. The total duration of the experiment (in hours) shown on the x-axis, and concentrations (in mM) of the substrate (D-gluconate), and product (2,3-KDG) stated on the y-axis. The initial concentration of D-gluconate in the reaction mixture was 50 mL. During this time, the substrate concentration remains the same, and there is no detectable activity of the product, which tells us where no substrate-to-product conversion is.

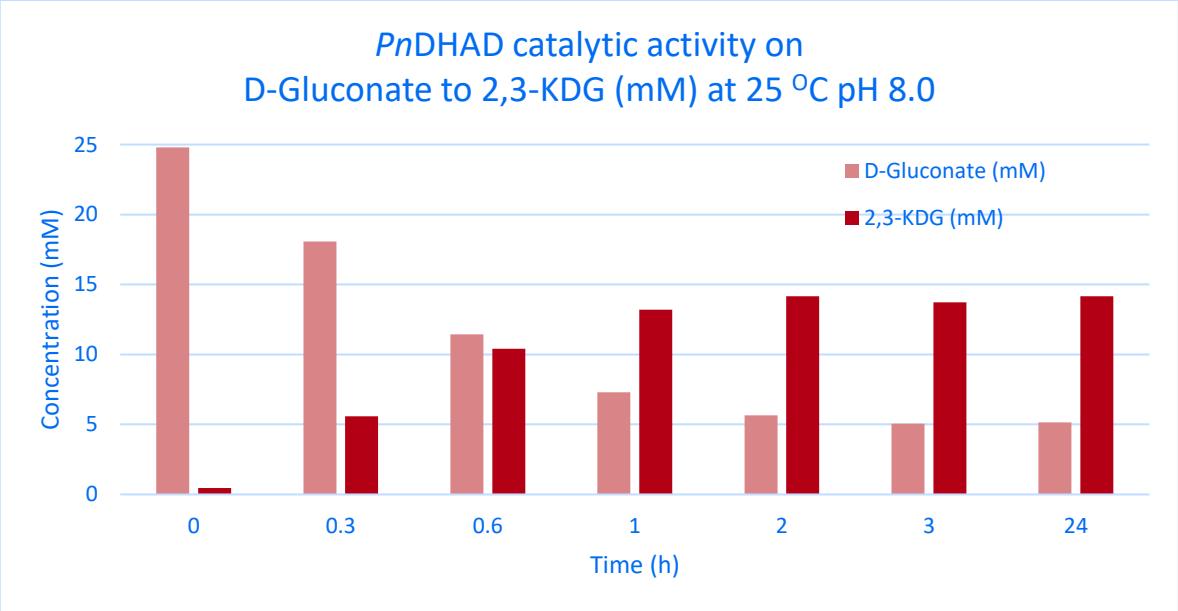

Figure 4. *Pn*DHAD 19IlvD catalytic activity on D-Gluconate to 2,3-KDG (mM) at 25°C pH 8.0.

The data shown in the **Figure 4** corresponds to the results of the second enzymatic activity assay. The total duration of the experiment (in hours) shown on the x-axis, and concentrations (in mM) of the substrate (D-gluconate), and product (2,3-KDG) stated on the y-axis. The initial concentration of D-gluconate in the reaction mixture was 50 mL. During the first experimental hour, the concentration of the substrate remains is half reduced and converted into the product, which tells us what 19IlvD enzyme is active on this specific substrate in these specific conditions. After one hour of the experiment, there are no detectable changes in substrate/product concentration.

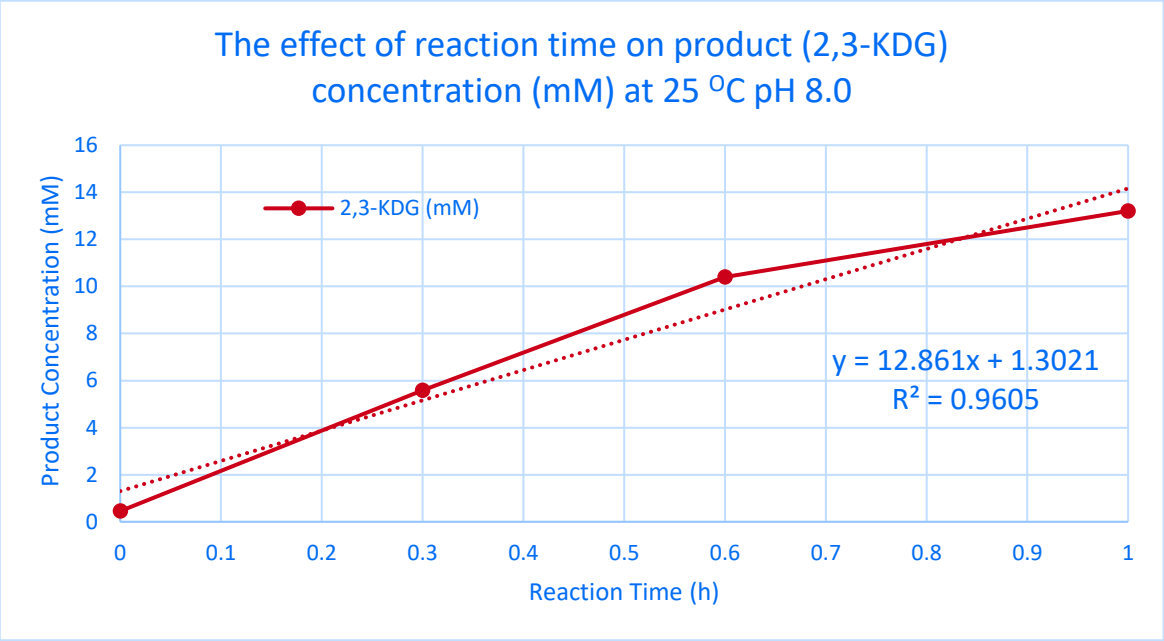

Figure 5. The effect of reaction time on product (2,3-KDG) concentration (mM) at 25°C pH 8.0.

The graph in the **Figure 5** shows the production rate of the 2,3-KDG during one hour of the reaction. The slope of the reaction corresponds to the amount of substrate converted into the product in one hour time – 12.861(mmol/h). R^2 is a correlation factor.

3.3 DISCUSSION AND FUTURE PLANS

Our experimental work started with cloning three dehydratase genes into the pET 28-a vector to transform them into *E. coli* cells, purify and test on the alternative substrate to detect their enzymatic activity. Once Sanger sequencing results arrived, DNA and amino acid sequencing of each of three enzymes (11IlvD, 17IlvD and 19IlvD) inserted into the pET 28-a vector were analysed. Results show that only the 19IlvD gene was cloned correctly into the pET 28-a plasmid. An amino acid sequence of 19IlvD was correct (was similar to the initial 19IlvD sequence from the National Center for Biotechnology Information (NCBI), while sequences of vectors with 11IlvD and 17IlvD were unclear. Furthermore, due to limited time, all activity assay experiments were carried out only for the 19IlvD samples.

Both activity assay experiments show that the 19IlvD enzyme was inactive on D-gluconate at 37^{O}C at pH 8.0 and active on the same alternative substrate at 25^{O}C at the same pH conditions. There are a couple of reasons for that. Firstly, before the first activity assay experiment, the autoinduction media, used for the protein expression, included Trace elements solution, one of which is iron. Most likely, the concentration of iron was smaller than the enzyme needed to bind the substrate and start converting it into the product. It has been shown that dehydratases, containing iron-sulfur cluster, need a metal ion as a co-factor to their activity (Rahman *et al.*, 2017). Another reason for the 19IlvD enzyme being inactive is the improper temperature setup. The temperature of 37 ^{O}C might be too high to allow the enzyme to be active. There is also an option that a combination of two previously described factors leads to the inactivity of the enzyme. Hence, to test this theory, before the second activity assay, 19IlvD enzymes were expressed in autoinduction media, containing 1M $FeCl_2$ to increase the concentration of the enzyme being expressed. Also, the temperature setup was lowered for the second activity assay experiment. The reaction mixture was incubated at 25 ^{O}C. Furthermore, the total experiment duration was extended to 24 hours, while the first experiment was conducted only for 3 hours to evaluate if enzyme activity is just exceptionally low and the substrate-to-product conversion process takes longer. Eventually, 19IlvD showed activity during the second experiment. Enzyme converted about half of the initial concentration of the substrate into the product of interest in just one hour but then became inactive. For the future work it is worth exploring the possibility of extending dehydratase activity by adding $FeCl_2$ in the reaction mixture during the experiment. The calculated specific activity of the enzyme was 6.85 μmol/min/mg, which is intriguing on an industry level but the life-time of the enzyme would need to me improved. Even if the 19IlvD

enzyme is capable of producing the expensive product of interest from the cheap alternative substrate, the production costs will remain relatively high as enzyme would need to be added at an hourly interval. There is a need to keep track of the concentration of enzymes. Without optimising the production environment, to produce high amounts of 2,3-KDG, enzymes will be needed to be added to the reaction every hour to keep the production rate high and stable. To make the 19IlvD considerable for industrial purposes, the enzyme should be tested on other alternative substrates with various pH levels, temperatures, substrate concentrations, and co-factors to find the most suitable conditions for fast and cheap biofuel production.

Our plans include optimising the 19IlvD enzyme to establish the best activity conditions. The enzyme needs to be tested on several alternative substrates with different temperatures and conditions. Once environmental *in vitro* conditions for a highly active enzyme are optimised, it can be further investigated for industrial purposes.

SUMMARY

In this work, we isolated, cloned, expressed, and purified a dihydroxy-acid dehydratase (DHAD) from the IlvD family from *Polaromonas naphthalenivorans* – 19IlvD –to examine its enzymatic activity in the alternative substrate – D-gluconate. The enzyme of interest was cloned into the pET 28-a vector. Then the vector containing the gene of interest was transformed into *E. coli* Turbo cell strain to achieve a high number of recombinant plasmids. Later, to achieve a high rate of protein expression, recombinant plasmids were transformed into BL21-DE3s and expressed with the presence of autoinduction media. Once 19IlvD was purified, two enzyme activity experiments were performed.

The results of the activity assays showed the 19IlvD enzyme was inactive on D-gluconate at 37 ^{O}C at pH 8.0 and active on the same alternative substrate at 25 ^{O}C at pH 8.0 in HEPES buffer. Half of the D-gluconate was converted into 2,3-KDG during the first hour of the second experiment. 19IlvD enzyme showed a specific activity of 6.85 μmol/min/mg. However, it became catalytically less active after one hour. During the second hour of the enzyme reaction time, the specific activity drops from 6.85 μmol/min/mg to 0.51 μmol/min/mg. Inactivity of the enzyme occurs between hours 2 and 3 with no measurable activity through 24 hours.

The enzymatic activity needs further investigation, such as enzyme needs to be tested on different alternative substrates with various pH conditions. The establishment of the optimized enzymatic activity will enable further investigation of the IlvD enzyme family in renewable biofuel production.

ACKNOWLEDGMENTS

I want to thank all my closest friends and family members for their unconditional love and emotional support during the whole period of my studies.

I would like to thank my supervisor Scott Bottoms for his guidance and help during my thesis work process.

Additionally, I would like to express my deepest gratitude to Associate professor Ilona Faustova for her constant support and encouragement throughout most challenging times.

Also, I want to thank Artemi Maljavin for guiding and mentoring our studies.

Last, but not least, I would like to thank Ekaterina Sedykh for being the best academic tutor I have ever had.

REFERENCES

About the Secretariat | UNFCCC. (n.d.). Retrieved May 27, 2022, from https://unfccc.int/about-us/about-the-secretariat

Alternative Fuels Data Center: Renewable Hydrocarbon Biofuels. (n.d.). Retrieved May 27, 2022, from https://afdc.energy.gov/fuels/emerging_hydrocarbon.html

Baroš, P., Matějovský, L., Macák, J., Staš, M., & Pospíšil, M. (2022). Corrosion Aggressiveness of Ethanol-Gasoline and Butanol-Gasoline Blends on Steel: Application of Electrochemical Impedance Spectroscopy. *Energy and Fuels*, *36*(5), 2616–2629. https://doi.org/10.1021/ACS.ENERGYFUELS.1C03680/ASSET/IMAGES/MEDIUM/EF1C03680_0012.GIF

Brito Cruz, C. H., Mendes Souza, G., & Barbosa Cortez, L. A. (2014). Biofuels for Transport. *Future Energy: Improved, Sustainable and Clean Options for Our Planet*, 215–244. https://doi.org/10.1016/B978-0-08-099424-6.00011-9

Brownstein, A. M. (2015). Isobutanol. *Renewable Motor Fuels*, 47–56. https://doi.org/10.1016/B978-0-12-800970-3.00005-4

Caspi, R., Billington, R., Fulcher, C. A., Keseler, I. M., Kothari, A., Krummenacker, M., Latendresse, M., Midford, P. E., Ong, Q., Ong, W. K., Paley, S., Subhraveti, P., & Karp, P. D. (2018). The MetaCyc database of metabolic pathways and enzymes. *Nucleic Acids Research*, *46*(D1), D633–D639. https://doi.org/10.1093/NAR/GKX935

Chen, H. (2015). Lignocellulose biorefinery feedstock engineering. *Lignocellulose Biorefinery Engineering*, 37–86. https://doi.org/10.1016/B978-0-08-100135-6.00003-X

Circular Economy | UNCTAD. (n.d.). Retrieved May 27, 2022, from https://unctad.org/topic/trade-and-environment/circular-economy

Dahman, Y., Dignan, C., Fiayaz, A., & Chaudhry, A. (2019). An introduction to biofuels, foods, livestock, and the environment. *Biomass, Biopolymer-Based Materials, and Bioenergy: Construction, Biomedical, and Other Industrial Applications*, 241–276. https://doi.org/10.1016/B978-0-08-102426-3.00013-8

Demirel, Y. (2018). 1.22 Biofuels. *Comprehensive Energy Systems*, *1–5*, 875–908. https://doi.org/10.1016/B978-0-12-809597-3.00125-5

Elobeid, A., Tokgoz, S., Hayes, D. J., Babcock, B. A., & Hart, C. E. (2006). *The Long-Run Impact of Corn-Based Ethanol on the Grain, Oilseed, and Livestock Sectors: A Preliminary Assessment*. www.card.iastate.edu

ENZYME - 4.2.1.9 Dihydroxy-acid dehydratase. (n.d.). Retrieved May 27, 2022, from https://enzyme.expasy.org/EC/4.2.1.9

Gao, H., Azam, T., Randeniya, S., Couturier, J., Rouhier, N., & Johnson, M. K. (2018). Function and maturation of the Fe–S center in dihydroxyacid dehydratase from Arabidopsis. *Journal of Biological Chemistry*, *293*(12), 4422–4433. https://doi.org/10.1074/JBC.RA117.001592

Geleynse, S., Brandt, K., Garcia-Perez, M., Wolcott, M., & Zhang, X. (2018). The Alcohol-to-Jet Conversion Pathway for Drop-In Biofuels: Techno-Economic Evaluation. *ChemSusChem*, *11*(21), 3728–3741. https://doi.org/10.1002/CSSC.201801690

Gutiérrez-Antonio, C., Romero-Izquierdo, A. G., Gómez-Castro, F. I., & Hernández, S. (2021). Production processes from lignocellulosic feedstock. *Production Processes of Renewable Aviation Fuel*, 129–169. https://doi.org/10.1016/B978-0-12-819719-6.00005-5

Harris, R. A. (2013). Glycolysis Overview. *Encyclopedia of Biological Chemistry: Second Edition*, 443–447. https://doi.org/10.1016/B978-0-12-378630-2.00044-X

Imlay, J. A. (2006). Iron-sulphur clusters and the problem with oxygen. *Molecular Microbiology*, *59*(4), 1073–1082. https://doi.org/10.1111/J.1365-2958.2006.05028.X

Jeon, C. O., Park, W., Ghiorse, W. C., & Madsen, E. L. (2004). Polaromonas naphthalenivorans sp. nov., a naphthalene-degrading bacterium from naphthalene-contaminated sediment. *International Journal of Systematic and Evolutionary Microbiology*, *54*(1), 93–97. https://doi.org/10.1099/IJS.0.02636-0/CITE/REFWORKS

Jiang, Y., Liu, W., Cheng, T., Cao, Y., Zhang, R., & Xian, M. (2015). Characterization of D-xylonate dehydratase YjhG from Escherichia coli. *Http://Dx.Doi.Org/10.1080/21655979.2015.1040208*, *6*(4), 227–232. https://doi.org/10.1080/21655979.2015.1040208

Kang, A., & Lee, T. S. (2015). Converting Sugars to Biofuels: Ethanol and Beyond. *Bioengineering 2015, Vol. 2, Pages 184-203*, *2*(4), 184–203. https://doi.org/10.3390/BIOENGINEERING2040184

Krishnan, S., Ahmad, M. F., Zainuddin, N. A., Din, M. F. M., Rezania, S., Chelliapan, S., Taib, S. M., Nasrullah, M., & Wahid, Z. A. (2020). Bioethanol production from lignocellulosic biomass (water hyacinth): a biofuel alternative. *Bioreactors: Sustainable Design and Industrial Applications in Mitigation of GHG Emissions*, 123–143. https://doi.org/10.1016/B978-0-12-821264-6.00009-7

Lakshmi, N. M., Binod, P., Sindhu, R., Awasthi, M. K., & Pandey, A. (2021). Microbial engineering for the production of isobutanol: current status and future directions. *Https://Doi.Org/10.1080/21655979.2021.1978189*, *12*(2), 12308–12321. https://doi.org/10.1080/21655979.2021.1978189

Mohr, A., & Raman, S. (2013). Lessons from first generation biofuels and implications for the sustainability appraisal of second generation biofuels. *Energy Policy*, *63*, 114. https://doi.org/10.1016/J.ENPOL.2013.08.033

MVIS | MVIS OneHundred - A Circular Economy: Designing out Waste. (n.d.). Retrieved May 27, 2022, from https://www.mvis-indices.com/mvis-onehundred/a-circular-economy-designing-out-waste

MYERS, J. W. (1961). Dihydroxy acid dehydrase: an enzyme involved in the biosynthesis of isoleucine and valine. *The Journal of Biological Chemistry*, *236*, 1414–1418. https://doi.org/10.1016/s0021-9258(18)64188-2

Neves, S. A., & Marques, A. C. (2022). Drivers and barriers in the transition from a linear economy to a circular economy. *Journal of Cleaner Production*, *341*, 130865. https://doi.org/10.1016/J.JCLEPRO.2022.130865

Noda, S., Mori, Y., Oyama, S., Kondo, A., Araki, M., & Shirai, T. (2019). Reconstruction of metabolic pathway for isobutanol production in Escherichia coli. *Microbial Cell Factories*, *18*(1), 124. https://doi.org/10.1186/S12934-019-1171-4/TABLES/3

Peralta-Yahya, P. P., Zhang, F., del Cardayre, S. B., & Keasling, J. D. (2012). Microbial engineering for the production of advanced biofuels. *Nature 2012 488:7411*, *488*(7411), 320–328. https://doi.org/10.1038/nature11478

pyruvate fermentation to isobutanol (engineered) | Pathway - PubChem. (n.d.). Retrieved May 27, 2022, from https://pubchem.ncbi.nlm.nih.gov/pathway/BioCyc:META_PWY-7111

Rahman, M. M., Andberg, M., Thangaraj, S. K., Parkkinen, T., Penttilä, M., Jänis, J., Koivula, A., Rouvinen, J., & Hakulinen, N. (2017). The Crystal Structure of a Bacterial l -Arabinonate Dehydratase Contains a [2Fe-2S] Cluster. *ACS Chemical Biology*, *12*(7), 1919–1927. https://doi.org/10.1021/acschembio.7b00304

Sherkhanov, S., Korman, T. P., Chan, S., Faham, S., Liu, H., Sawaya, M. R., Hsu, W. T., Vikram, E., Cheng, T., & Bowie, J. U. (2020). Isobutanol production freed from biological limits using synthetic biochemistry. *Nature Communications 2020 11:1*, *11*(1), 1–10. https://doi.org/10.1038/s41467-020-18124-1

Singh, A., Chaudhary, S., Shankar, A., & Prasad, V. (2019). Polyketide and Its Derivatives. *New and Future Developments in Microbial Biotechnology and Bioengineering: Microbial Genes Biochemistry and Applications*, 219–227. https://doi.org/10.1016/B978-0-444-63503-7.00013-9

The Paris Agreement | UNFCCC. (n.d.). Retrieved May 27, 2022, from https://unfccc.int/process-and-meetings/the-paris-agreement/the-paris-agreement

Wess, J., Brinek, M., & Boles, E. (2019). Improving isobutanol production with the yeast Saccharomyces cerevisiae by successively blocking competing metabolic pathways as well as ethanol and glycerol formation. *Biotechnology for Biofuels*, *12*(1), 1–15. https://doi.org/10.1186/S13068-019-1486-8/TABLES/4

What is the Kyoto Protocol? | UNFCCC. (n.d.). Retrieved May 27, 2022, from https://unfccc.int/kyoto_protocol

NON-EXCLUSIVE LICENCE TO REPRODUCE THESIS AND MAKE THESIS PUBLIC

I, Mariia Novoshinskaia

grant the University of Tartu a free permit (non-exclusive licence) to

reproduce, for the purpose of preservation, including for adding to the DSpace digital archives until the expiry of the term of copyright, my thesis

Characterization of a Novel Dehydratase from the Polycyclic Aromatic Hydrocarbon (PAH) Consuming Microbe, Polaromonas naphthalenivorans

supervised by Scott Bottoms

2. I grant the University of Tartu a permit to make the thesis specified in point 1 available to the public via the web environment of the University of Tartu, including via the DSpace digital archives, under the Creative Commons licence CC BY NC ND 4.0, which allows, by giving appropriate credit to the author, to reproduce, distribute the work and communicate it to the public, and prohibits the creation of derivative works and any commercial use of the work until the expiry of the term of copyright.

3. I am aware of the fact that the author retains the rights specified in points 1 and 2.

4. I confirm that granting the non-exclusive licence does not infringe other persons' intellectual property rights or rights arising from the personal data protection legislation.

Mariia Novoshinskaia

30/05/2022